

---

1 **ARTICLE**

---

2 **Comparison of theoretical formulae and bootstrap method**  
3 **for statistical error estimation of Feynman- $\alpha$  method**

4 Tomohiro Endo<sup>a\*</sup>, Akio Yamamoto<sup>a</sup>

5 <sup>a</sup> *Graduate School of Engineering, Nagoya University, Furo-cho, Chikusa-ku, Nagoya*  
6 *464-8603, Japan;*

7  
8 **Abstract**

9 This paper discusses the statistical error of the variance-to-mean ratio, or the  $Y$  value in the  
10 Feynman- $\alpha$  method, from a single measurement of reactor noise. As a theoretical approach,  
11 two practical theoretical formulae are derived to estimate the statistical error of  $Y$ : one is  
12 based on the propagation of uncertainty with unbiased estimators for the third- and  
13 fourth-order central moments; the other is a simplified formula that reuses the  $Y$  value under  
14 the fundamental mode approximation, where the subcriticality is approximately less than  
15 10,000 pcm. As a numerical approach, the bootstrap method is improved to efficiently  
16 estimate the correlations of  $Y$  between different counting gate widths, or covariance matrix  
17  $\Sigma_Y$ , due to the bunching method. Through an actual reactor noise experiment at the Kyoto  
18 University Criticality Assembly, the statistical errors of  $Y$  using the theoretical formulae and  
19 the bootstrap method are validated by comparing the reference statistical errors that are  
20 estimated from the multiple experiments of reactor noise. Furthermore, the impact of  $\Sigma_Y$  on  
21 the statistical error of the prompt neutron decay constant  $\alpha$  is numerically investigated.  
22 Consequently, in the case of this experimental analysis, it was confirmed that the bootstrap  
23 method with the correlations of  $Y$  seems to be slightly better from the viewpoint of the  
24 coverage probability of the estimated confidence intervals of  $\alpha$ , although the fitting error  
25 method without the correlation of  $Y$  could be useful for the order estimation of the statistical  
26 error of  $\alpha$ .

---

\*Corresponding author. Email: t-endo@energy.nagoya-u.ac.jp

1

2 *Keywords; Feynman- $\alpha$  method, statistical error, covariance, bootstrap method, prompt*  
3 *neutron decay constant*

4

5

6 **Highlights**

7 ✓ Estimation formulae for statistical error of variance-to-mean ratio  $Y$  are derived.

8 ✓ Statistical error of  $Y$  can be estimated by reusing  $Y$  without higher-order moments.

9 ✓ Bootstrap method enables covariance estimation of  $Y$  between counting gate widths.

10 ✓ Covariance is useful in better error-estimation of prompt neutron decay constant.

## 1    **1. Introduction**

2            The study of subcriticality monitoring is important to achieve safe and efficient operation  
3 and management in nuclear fuel-related facilities. It is also important for the  
4 Accelerator-Driven System (ADS), where the subcritical state must be maintained during  
5 operation [1,2]. Furthermore, in the retrieval of fuel debris from Fukushima Daiichi units 1–3  
6 with the submersion condition, there is a possibility of a positive reactivity insertion event due  
7 to the change in the moderation ratio; thus, subcriticality monitoring to prevent recriticality is  
8 an important issue [3].

9            The Feynman- $\alpha$  method, also called the variance-to-mean ratio method, is a practical  
10 subcriticality measurement technique based on the zero-power reactor noise analysis [4,5,6,7].  
11 Using the Feynman- $\alpha$  method, the prompt neutron decay constant  $\alpha$  can be measured by  
12 analyzing the time-series data of neutron counts; then the measurement value of  $\alpha$  is  
13 converted to the subcriticality  $-\rho \equiv (1 - k_{\text{eff}})/k_{\text{eff}}$ , which is the absolute value of the  
14 negative reactivity. In the Feynman- $\alpha$  method, quantification of the statistical error of the  
15 variance-to-mean ratio (or  $Y$  value) is useful information for clarifying the measurement  
16 precision and reconsidering the measurement time if necessary. For example, if the estimated  
17 statistical error is unacceptable and should be reduced by half, the central limit theorem  
18 implies that four times the measurement time is necessary. Here, one of the simple estimation  
19 methods for the statistical error  $\sigma_Y$  is multiple measurements of reactor noise; however, an  
20 additional longer measurement time is needed to repeat the multiple times of measurements  
21 for the error estimation.

22            Thus, in our previous study, the statistical error estimation technique using only a single  
23 measurement of reactor noise, *i.e.*, without multiple measurements, was proposed using the  
24 bootstrap method [8,9]. In the bootstrap method, the statistical error can be simply estimated  
25 by a resampling that is based on an experimentally inferred probability distribution of neutron  
26 count. It is worth noting that the calculation time is long due to the resampling.

1 As another approach, we newly propose theoretical formulae to efficiently estimate the  
2 statistical error  $\sigma_Y$  for a single measurement. Compared with the previous theoretical  
3 investigations [10,11,12,13], the following points are the remarkable features of our present  
4 work:

- 5 1. In the propagation of uncertainty for the statistical error of  $Y$ , the covariance between  
6 the sample mean and the unbiased variance is explicitly considered.
- 7 2. Unbiased estimators for central moments are utilized.
- 8 3. Under the fundamental mode approximation where  $-\rho < 10,000$  pcm, a more  
9 simplified formula for  $\sigma_Y$  by reusing  $Y$  is also derived.

10 In the theoretical approach, however, correlations of  $Y$  between different counting gate  
11 widths  $T$  (or covariance matrix  $\Sigma_Y$ ), which originate from the bunching method for the same  
12 time-series data [14], are an unresolved issue. Therefore, to numerically investigate the impact  
13 of  $\Sigma_Y$  on the statistical error of  $\alpha$  in the fitting process, we improve procedures in the  
14 bootstrap method to effectively estimate the bootstrap covariance matrix  $\Sigma_{Y^*}$ .

15 One of the major aims of this study is to validate the statistical errors of  $Y$  and  $\alpha$  that  
16 are obtained from a single measurement of reactor noise, by comparing them with the  
17 reference statistical errors or by evaluating the coverage probability of the estimated  
18 confidence interval. Here, the reference statistical errors and the coverage probability can be  
19 evaluated using the multiple experiments of reactor noise. Through this validation, we aim to  
20 confirm whether the estimated statistical errors are reasonable, *i.e.*, neither overestimated nor  
21 underestimated. The reduction of statistical errors of  $Y$  and  $\alpha$  is out of scope of this study.

22 The rest of the paper is structured as follows. In Section 2, the theory of statistical error  
23  $\sigma_Y$  is described. In Section 3, we explain the improved bootstrap method. In Section 4, the  
24 derived estimation formulae and the improved bootstrap method are demonstrated through an  
25 experimental analysis for actual reactor noise data that were measured at the Kyoto University

1 Criticality Assembly (KUCA). In addition, the impact of  $\Sigma_Y$  on the statistical error of  $\alpha$  in  
 2 the fitting process is discussed. Finally, in Section 5, concluding remarks are presented.

3

## 4 **2. Theory for statistical error of $Y$ value**

### 5 **2.1. Propagation of uncertainty for $Y$ value**

6 Let us assume a steady state of a source-driven subcritical system. In this subcritical  
 7 system, neutron counts  $C_i(T)$  are measured  $N$  times ( $1 \leq i \leq N$ ), where  $T$  is the counting  
 8 gate width and  $N$  is the total number of count data. Then, the second-order  
 9 neutron-correlation value  $Y$  is evaluated as the variance-to-mean ratio:

$$Y \equiv \frac{\sigma^2}{\langle C \rangle} - 1 \approx \frac{s^2}{\bar{C}} - 1, \quad (1)$$

$$\sigma^2 \equiv \langle (C - \langle C \rangle)^2 \rangle, \quad (2)$$

10 where the bracket  $\langle \rangle$  indicates the expected value;  $\langle C \rangle$  and  $\sigma^2$  are the population mean and  
 11 variance of neutron counts; and  $\bar{C}$  and  $s^2$  represent the sample mean and the unbiased  
 12 variance of  $C_i(T)$ , respectively:

$$\bar{C} = \frac{1}{N} \sum_{i=1}^N C_i, \quad (3)$$

$$s^2 = \frac{1}{N-1} \sum_{i=1}^N (C_i - \bar{C})^2. \quad (4)$$

13 Note that the notation  $T$  is omitted in Eqs. (1)–(4) for simplicity.

14 Based on the propagation of uncertainty (or the sandwich rule) for Eq. (1), the statistical  
 15 error  $\sigma_Y$  can be estimated as follows:

$$\begin{aligned} \sigma_Y &\approx \sqrt{\left(\frac{\partial Y}{\partial \sigma_{\bar{C}}} \sigma_{\bar{C}}\right)^2 + \left(\frac{\partial Y}{\partial s^2} \sigma_{s^2}\right)^2 + 2 \frac{\partial Y}{\partial \sigma_{\bar{C}}} \frac{\partial Y}{\partial s^2} \text{cov}(\bar{C}, s^2)} \\ &= (Y + 1) \sqrt{\left(-\frac{\sigma_{\bar{C}}}{\bar{C}}\right)^2 + \left(\frac{\sigma_{s^2}}{s^2}\right)^2 - 2 \frac{\text{cov}(\bar{C}, s^2)}{\bar{C} s^2}}, \end{aligned} \quad (5)$$

1 where  $\sigma_{\bar{C}}$  and  $\sigma_{s^2}$  are the statistical errors of  $\bar{C}$  and  $s^2$ , respectively; and  $\text{cov}(\bar{C}, s^2)$  is  
 2 the covariance between  $\bar{C}$  and  $s^2$ . In Eq. (5), the expected values of  $\sigma_{\bar{C}}$ ,  $\sigma_{s^2}$ , and  
 3  $\text{cov}(\bar{C}, s^2)$  can be derived as follows [15]:

$$\langle \sigma_{\bar{C}} \rangle = \sqrt{\frac{\sigma^2}{N}}, \quad (6)$$

$$\langle \sigma_{s^2} \rangle = \sqrt{\frac{1}{N} \left( \mu_4 - \frac{N-3}{N-1} (\sigma^2)^2 \right)}, \quad (7)$$

$$\langle \text{cov}(\bar{C}, s^2) \rangle = \frac{\mu_3}{N}, \quad (8)$$

$$\mu_3 \equiv \langle (C - \langle C \rangle)^3 \rangle, \quad (9)$$

$$\mu_4 \equiv \langle (C - \langle C \rangle)^4 \rangle, \quad (10)$$

4 where  $\mu_3$  and  $\mu_4$  correspond to the third- and fourth-order central moments, respectively. If  
 5 the same time-series data are used for the estimation of both  $\bar{C}$  and  $s^2$ , the covariance term  
 6  $\text{cov}(\bar{C}, s^2)$  should not be neglected in Eq. (5).

7

## 8 **2.2. Estimation formula using unbiased estimators for central moments**

9 As can be seen from Eqs. (5)–(8), it is necessary for the estimation of the statistical error  
 10  $\sigma_Y$  to appropriately evaluate the third- and fourth-order central moments  $\mu_3$  and  $\mu_4$  from  
 11 the finite number of neutron count data  $C_i(T)$  ( $1 \leq i \leq N$ ).

12 For this purpose,  $\mu_3$  and  $\mu_4$  can be estimated using the unbiased estimators  $h_3$  and  
 13  $h_4$  in the h-statistics, respectively [16], where  $h_3$  and  $h_4$  are obtained by

$$h_3 = \frac{N}{(N-1)(N-2)} \sum_{i=1}^N (C_i - \bar{C})^3, \quad (11)$$

$$h_4 = \frac{N^2 - 2N + 3}{(N-1)(N-2)(N-3)} \sum_{i=1}^N (C_i - \bar{C})^4 - \frac{3(2N-3)}{N(N-1)(N-2)(N-3)} \left( \sum_{i=1}^N (C_i - \bar{C})^2 \right)^2. \quad (12)$$

1 Using the unbiased estimators  $s^2$ ,  $h_3$ , and  $h_4$  in Eqs. (5)–(8) instead of  $\sigma^2$ ,  $\mu_3$ , and  $\mu_4$ , the  
 2 statistical error  $\sigma_{Y,h}$  can be evaluated by the following formula:

$$\sigma_{Y,h} \approx (Y + 1) \sqrt{\frac{Y + 1}{N\bar{C}} + \frac{1}{N} \left( \frac{h_4}{(s^2)^2} - \frac{N-3}{N-1} \right) - \frac{2h_3}{N\bar{C}s^2}}. \quad (13)$$

3 In the conventional Feynman- $\alpha$  method, the calculations of  $\bar{C}$  and  $s^2$  are sufficient for the  
 4 evaluation of the  $Y$  value as defined in Eq. (1). For the estimation of  $\sigma_{Y,h}$  by Eq. (13),  
 5 additional calculations of  $h_3$  and  $h_4$  are necessary.

6

### 7 **2.3. Simplified formula by reusing the second-order neutron-correlation**

8 In general, the magnitude of the  $n$ th-order neutron-correlation is proportional to the  
 9  $(n-1)$ th power of the detector importance function, or detection efficiency [17,18,19]. For  
 10 example, if  $Y < 1$ , it is expected that the third and fourth-order neutron-correlations are  
 11 lower than the second-order neutron-correlation. In particular, in the case of  $Y \ll 1$ , it was  
 12 clarified that the probability density function of the neutron count can be sufficiently  
 13 approximated by the negative binomial distribution [7,10,11]. If the negative binomial  
 14 distribution approximation is applicable, the statistical error  $\sigma_Y$  can be approximately  
 15 estimated only using  $\langle C \rangle$  and  $Y$  [10]. Although the negative binomial distribution  
 16 approximation is useful for estimating  $\sigma_Y$ , the applicability depends on experimental  
 17 conditions, *e.g.*, low detection efficiency and/or deep subcritical system. Thus, in this  
 18 subsection, a more simplified formula of the statistical error  $\sigma_Y$  is newly derived without  
 19 depending on the magnitude of  $Y$ , on the basis of the fundamental mode approximation  
 20 where  $0.9 < k_{\text{eff}} < 1$ , or  $-\rho < 10,000$  pcm.

1  
2  
3  
4  
5  
6  
7  
8  
9  
10  
11  
12  
13  
14  
15  
16  
17  
18

In the steady state of the source-driven subcritical system, a master equation for probability-generating functions of neutron count is described as follows [7,18]:

$$\ln(G(Z, T|S)) = \int_0^\infty du \int_V dV S(\vec{r}) \sum_{q=0}^\infty p_s(q, \vec{r}) \{(\bar{g}(Z, T|\vec{r}, u))^q - 1\}, \quad (14)$$

$$G(Z, T|S) \equiv \sum_{C=0}^\infty Z^C P(C, T|S), \quad (15)$$

$$\bar{g}(Z, T|\vec{r}, u) \equiv \int_0^\infty dE \int_{4\pi} d\Omega \frac{\chi_s(\vec{r}, E)}{4\pi} g(Z, T|\vec{r}, E, \vec{\Omega}, u), \quad (16)$$

$$g(Z, T|\vec{r}, E, \vec{\Omega}, u) \equiv \sum_{C=0}^\infty Z^C p(C, T|\vec{r}, E, \vec{\Omega}, u), \quad (17)$$

where

$p(C, T|\vec{r}, E, \vec{\Omega}, u)$  : probability that  $C$  neutrons are detected during the counting gate width  $T$  due to a neutron at  $(\vec{r}, E, \vec{\Omega}, u)$ , where  $u$  is a backward time-variable, *i.e.*,  $u \equiv -t$ ,  $u = 0$  corresponds to the counting gate closing time;

$g(Z, T|\vec{r}, E, \vec{\Omega}, u)$  : probability-generating function for  $p(C, T|\vec{r}, E, \vec{\Omega}, u)$ , where  $Z$  is the variable of generating function;

$\bar{g}(Z, T|\vec{r}, u)$  : weighted mean of probability generating function, of which weighting function is  $\frac{\chi_s(\vec{r}, E)}{4\pi}$ ;

$P(C, T|S)$  : probability that  $C$  neutrons are detected during the counting gate width  $T$  owing to a stationary external neutron source  $S$ ;

$G(Z, T|S)$  : probability-generating function for  $P(C, T|S)$ .

$S(\vec{r})$  : spatial distribution of source strength for the external neutron source;

$\chi_s(\vec{r}, E)$  : energy spectrum of the external neutron source;

$p_s(q, \vec{r})$  : probability that  $q$  neutrons are emitted per decay of the external source.



1 Using the mathematical properties of the probability-generating function  $G(Z, T|S)$   
 2 described by Eq. (14), the  $n$ th-order neutron-correlation value  $\mathcal{Y}_n$  ( $n \geq 2$ ) is defined as

$$\mathcal{Y}_n \equiv \frac{1}{\langle C \rangle} \frac{\partial^n}{\partial Z^n} \ln(G(Z, T|S)) \Big|_{Z=1}, \quad (18)$$

3 where  $\mathcal{Y}_2$  corresponds to the  $Y$  value in the Feynman- $\alpha$  method. For example, the first- to  
 4 fourth-order partial derivatives of  $\ln(G(Z, T|S))$  with respect to  $Z$  are shown below:

$$\frac{\partial(\ln G)}{\partial Z} = \frac{1}{G} \frac{\partial G}{\partial Z}, \quad (19)$$

$$\frac{\partial^2(\ln G)}{\partial Z^2} = \frac{1}{G} \frac{\partial^2 G}{\partial Z^2} - \left( \frac{\partial(\ln G)}{\partial Z} \right)^2, \quad (20)$$

$$\frac{\partial^3(\ln G)}{\partial Z^3} = \frac{1}{G} \frac{\partial^3 G}{\partial Z^3} - 3 \frac{\partial(\ln G)}{\partial Z} \frac{\partial^2(\ln G)}{\partial Z^2} - \left( \frac{\partial(\ln G)}{\partial Z} \right)^3, \quad (21)$$

$$\begin{aligned} \frac{\partial^4(\ln G)}{\partial Z^4} = & \frac{1}{G} \frac{\partial^4 G}{\partial Z^4} - 4 \frac{\partial(\ln G)}{\partial Z} \frac{\partial^3(\ln G)}{\partial Z^3} - 3 \left( \frac{\partial^2(\ln G)}{\partial Z^2} \right)^2 - 6 \left( \frac{\partial(\ln G)}{\partial Z} \right)^2 \frac{\partial^2(\ln G)}{\partial Z^2} \\ & - \left( \frac{\partial(\ln G)}{\partial Z} \right)^4, \end{aligned} \quad (22)$$

5 where arguments  $(Z, T|S)$  of  $G(Z, T|S)$  are omitted for simplicity. In addition,  $G(Z, T|S)$   
 6 satisfies the following mathematical properties:

$$G(Z, T|S) \Big|_{Z=1} = \sum_{C=0}^{\infty} P(C, T|S) = 1, \quad (23)$$

$$\frac{\partial^n G}{\partial Z^n} \Big|_{Z=1} = \left\langle \frac{C!}{(C-n)!} \right\rangle. \quad (24)$$

7 Using Eqs. (18)–(24), the second- to fourth-order neutron-correlation values can be  
 8 expressed as

$$Y \equiv \mathcal{Y}_2 = \frac{1}{\langle C \rangle} \frac{\partial^2(\ln G)}{\partial Z^2} \Big|_{Z=1} = \frac{\langle C(C-1) \rangle - \langle C \rangle^2}{\langle C \rangle}, \quad (25)$$

$$y_3 = \frac{1}{\langle C \rangle} \frac{\partial^3(\ln G)}{\partial Z^3} \Big|_{Z=1} = \frac{\langle C(C-1)(C-2) \rangle - 3Y\langle C \rangle^2 - \langle C \rangle^3}{\langle C \rangle}, \quad (26)$$

$$y_4 = \frac{1}{\langle C \rangle} \frac{\partial^4(\ln G)}{\partial Z^4} \Big|_{Z=1} = \frac{\langle C(C-1)(C-2)(C-3) \rangle - 4y_3\langle C \rangle^2 - 3Y^2\langle C \rangle^2 - 6Y\langle C \rangle^3 - \langle C \rangle^4}{\langle C \rangle}, \quad (27)$$

1

2 As reported in our previous studies [18,19], the saturation values of  $Y$ ,  $y_3$ , and  $y_4$  in

3 the limit of  $T \rightarrow \infty$  can be derived by differentiating the right-hand side of Eq. (14) and

4 using the first to fourth-order detector importance functions:

$$Y_\infty \equiv \lim_{T \rightarrow \infty} Y = \frac{\int_V S(\vec{r}) \sum_{q=0}^{\infty} p_s(q, \vec{r}) \{q\bar{I}_{2,s}^\dagger(\vec{r}) + q(q-1)(\bar{I}_{1,s}^\dagger(\vec{r}))^2\} dV}{\int_V S(\vec{r}) \sum_{q=0}^{\infty} p_s(q, \vec{r}) q\bar{I}_{1,s}^\dagger(\vec{r}) dV}, \quad (28)$$

$$y_{3,\infty} \equiv \lim_{T \rightarrow \infty} y_3 = \frac{\int_V S(\vec{r}) \sum_{q=0}^{\infty} p_s(q, \vec{r}) \left\{ q\bar{I}_{3,s}^\dagger(\vec{r}) + 3q(q-1)\bar{I}_{1,s}^\dagger(\vec{r})\bar{I}_{2,s}^\dagger(\vec{r}) + q(q-1)(q-2)(\bar{I}_{1,s}^\dagger(\vec{r}))^3 \right\} dV}{\int_V S(\vec{r}) \sum_{q=0}^{\infty} p_s(q, \vec{r}) q\bar{I}_{1,s}^\dagger(\vec{r}) dV}, \quad (29)$$

$$y_{4,\infty} \equiv \lim_{T \rightarrow \infty} y_4$$

$$= \frac{\int_V S(\vec{r}) \sum_{q=0}^{\infty} p_s(q, \vec{r}) \left\{ \begin{array}{l} q\bar{I}_{4,s}^\dagger(\vec{r}) + 4q(q-1)\bar{I}_{1,s}^\dagger(\vec{r})\bar{I}_{3,s}^\dagger(\vec{r}) \\ + 3q(q-1)(\bar{I}_{2,s}^\dagger(\vec{r}))^2 \\ + 6q(q-1)(q-2)(\bar{I}_{1,s}^\dagger(\vec{r}))^2\bar{I}_{2,s}^\dagger(\vec{r}) \\ + q(q-1)(q-2)(q-3)(\bar{I}_{1,s}^\dagger(\vec{r}))^4 \end{array} \right\} dV}{\int_V S(\vec{r}) \sum_{q=0}^{\infty} p_s(q, \vec{r}) q\bar{I}_{1,s}^\dagger(\vec{r}) dV}, \quad (30)$$

$$\bar{I}_{n,s}^\dagger(\vec{r}) \equiv \int_0^\infty dE' \int_{4\pi} d\Omega' \frac{\chi_s(\vec{r}, E')}{4\pi} I_n^\dagger(\vec{r}, E', \vec{\Omega}'), \quad (31)$$

5 where the subscript “ $\infty$ ” indicates the saturation values in the limit of  $T \rightarrow \infty$ ;  $\bar{I}_{n,s}^\dagger(\vec{r})$  is the

6 weighted mean of the  $n$ th-order detector importance function  $I_n^\dagger(\vec{r}, E, \vec{\Omega})$  that satisfies the

7 following adjoint neutron transport equations [18,19]:

$$\mathbf{B}^\dagger I_1^\dagger(\vec{r}, E, \vec{\Omega}) = \Sigma_d(\vec{r}, E), \quad (32)$$

$$\mathbf{B}^\dagger I_2^\dagger(\vec{r}, E, \vec{\Omega}) = \Sigma_f(\vec{r}, E) \sum_{\nu=0}^{\infty} p_f(\nu, \vec{r}) \nu(\nu-1) \left( \bar{I}_{1,f}^\dagger(\vec{r}) \right)^2, \quad (33)$$

$$\mathbf{B}^\dagger I_3^\dagger(\vec{r}, E, \vec{\Omega}) = \Sigma_f(\vec{r}, E) \sum_{\nu=0}^{\infty} p_f(\nu, \vec{r}) \begin{pmatrix} 3\nu(\nu-1) \bar{I}_{1,f}^\dagger(\vec{r}) \bar{I}_{2,f}^\dagger(\vec{r}) \\ + \nu(\nu-1)(\nu-2) \left( \bar{I}_{1,f}^\dagger(\vec{r}) \right)^3 \end{pmatrix}, \quad (34)$$

$$\begin{aligned} & \mathbf{B}^\dagger I_4^\dagger(\vec{r}, E, \vec{\Omega}) \\ &= \Sigma_f(\vec{r}, E) \sum_{\nu=0}^{\infty} p_f(\nu, \vec{r}) \begin{pmatrix} 4\nu(\nu-1) \bar{I}_{1,f}^\dagger(\vec{r}) \bar{I}_{3,f}^\dagger(\vec{r}) + 3\nu(\nu-1) \left( \bar{I}_{2,f}^\dagger(\vec{r}) \right)^2 \\ + 6\nu(\nu-1)(\nu-2) \left( \bar{I}_{1,f}^\dagger(\vec{r}) \right)^2 \bar{I}_{2,f}^\dagger(\vec{r}) \\ + \nu(\nu-1)(\nu-2)(\nu-3) \left( \bar{I}_{1,f}^\dagger(\vec{r}) \right)^4 \end{pmatrix}, \end{aligned} \quad (35)$$

$$\bar{I}_{n,f}^\dagger(\vec{r}) \equiv \int_0^\infty dE' \int_{4\pi} d\Omega' \frac{\chi_f(\vec{r}, E')}{4\pi} I_n^\dagger(\vec{r}, E', \vec{\Omega}'), \quad (36)$$

$$\mathbf{B}^\dagger \equiv \mathbf{A}^\dagger - \mathbf{F}^\dagger, \quad (37)$$

$$\mathbf{A}^\dagger \equiv -\vec{\Omega} \nabla + \Sigma_t(\vec{r}, E) - \int_0^\infty dE' \int_{4\pi} d\Omega' \Sigma_s(\vec{r}, E \rightarrow E', \vec{\Omega} \rightarrow \vec{\Omega}'), \quad (38)$$

$$\mathbf{F}^\dagger \equiv \nu \Sigma_f(\vec{r}, E) \int_0^\infty dE' \int_{4\pi} d\Omega' \frac{\chi_f(\vec{r}, E')}{4\pi}, \quad (39)$$

1 where the superscript “†” indicates the adjoint;  $\mathbf{B}^\dagger$ ,  $\mathbf{A}^\dagger$  and  $\mathbf{F}^\dagger$  are the adjoint Boltzman,  
2 the net neutron-loss, and the neutron-production operators, respectively;  $\Sigma_d(\vec{r}, E)$  is the  
3 macroscopic neutron-detection cross-section; and  $\chi_f(\vec{r}, E)$  is the energy spectrum of fission;  
4  $p_f(\nu, \vec{r})$  is the probability that  $\nu$  neutrons are emitted per fission; other notations maintain  
5 their conventional meanings in reactor physics.

6 Now, let us assume the fundamental mode approximation is applicable to  $I_n^\dagger(\vec{r}, E, \vec{\Omega})$ .  
7 This approximation is more reasonable under a subcritical condition where the effective  
8 neutron multiplication factor  $k_{\text{eff}}$  is closer to unity. Then, using the fundamental modes of

- 1 forward and adjoint  $k_{\text{eff}}$ -eigenfunctions, *i.e.*,  $\psi_0(\vec{r}, E, \vec{\Omega})$  and  $\psi_0^\dagger(\vec{r}, E, \vec{\Omega})$ ,  $I_n^\dagger(\vec{r}, E, \vec{\Omega})$  can  
 2 be approximated as follows:

$$I_1^\dagger(\vec{r}, E, \vec{\Omega}) \approx \frac{\mathcal{D}_0}{-\rho\mathcal{F}_1} \psi_0^\dagger(\vec{r}, E, \vec{\Omega}), \quad (40)$$

$$I_2^\dagger(\vec{r}, E, \vec{\Omega}) \approx \left( \frac{\mathcal{D}_0}{-\rho\mathcal{F}_1} \right)^2 \frac{\mathcal{F}_2}{-\rho\mathcal{F}_1} \psi_0^\dagger(\vec{r}, E, \vec{\Omega}), \quad (41)$$

$$I_3^\dagger(\vec{r}, E, \vec{\Omega}) \approx \left( \frac{\mathcal{D}_0}{-\rho\mathcal{F}_1} \right)^3 \left( 3 \left( \frac{\mathcal{F}_2}{-\rho\mathcal{F}_1} \right)^2 + \frac{\mathcal{F}_3}{-\rho\mathcal{F}_1} \right) \psi_0^\dagger(\vec{r}, E, \vec{\Omega}), \quad (42)$$

$$I_4^\dagger(\vec{r}, E, \vec{\Omega}) \approx \left( \frac{\mathcal{D}_0}{-\rho\mathcal{F}_1} \right)^4 \left( 15 \left( \frac{\mathcal{F}_2}{-\rho\mathcal{F}_1} \right)^3 + 10 \frac{\mathcal{F}_2\mathcal{F}_3}{(-\rho\mathcal{F}_1)^2} + \frac{\mathcal{F}_4}{-\rho\mathcal{F}_1} \right) \psi_0^\dagger(\vec{r}, E, \vec{\Omega}), \quad (43)$$

- 3 where parameters  $\mathcal{D}_0$  and  $\mathcal{F}_n$  are introduced for convenience as follows:

$$\mathcal{D}_0 \equiv \int_V dV \int_0^\infty dE \Sigma_d(\vec{r}, E) \phi_0(\vec{r}, E), \quad (44)$$

$$\mathcal{F}_n \equiv \int_V dV \int_0^\infty dE \Sigma_f(\vec{r}, E) \phi_0(\vec{r}, E) \sum_{v=0}^{\infty} \frac{v!}{(v-n)!} p_f(v, \vec{r}, E) \left( \bar{\psi}_{0,f}^\dagger(\vec{r}) \right)^n, \quad (45)$$

$$\phi_0(\vec{r}, E) \equiv \int_{4\pi} \psi_0(\vec{r}, E, \vec{\Omega}') d\Omega', \quad (46)$$

$$\bar{\psi}_{0,f}^\dagger(\vec{r}) \equiv \int_0^\infty dE' \int_{4\pi} d\Omega' \frac{\chi_f(\vec{r}, E')}{4\pi} \psi_0^\dagger(\vec{r}, E', \vec{\Omega}'). \quad (47)$$

- 4 Note that  $\psi_0(\vec{r}, E, \vec{\Omega})$  and  $\psi_0^\dagger(\vec{r}, E, \vec{\Omega})$  satisfy the following forward and adjoint  
 5  $k_{\text{eff}}$ -eigenvalue equations, respectively:

$$\mathbf{A}\psi_0(\vec{r}, E, \vec{\Omega}) = \frac{1}{k_{\text{eff}}} \mathbf{F}\psi_0(\vec{r}, E, \vec{\Omega}), \quad (48)$$

$$\mathbf{A}^\dagger\psi_0^\dagger(\vec{r}, E, \vec{\Omega}) = \frac{1}{k_{\text{eff}}} \mathbf{F}^\dagger\psi_0^\dagger(\vec{r}, E, \vec{\Omega}), \quad (49)$$

$$\mathbf{A} \equiv \vec{\Omega} \nabla + \Sigma_t(\vec{r}, E) - \int_0^\infty dE' \int_{4\pi} d\Omega' \Sigma_s(\vec{r}, E' \rightarrow E, \vec{\Omega}' \rightarrow \vec{\Omega}), \quad (50)$$

$$\mathbf{F} \equiv \frac{\chi_f(\vec{r}, E)}{4\pi} \int_0^\infty dE' \int_{4\pi} d\Omega' \nu \Sigma_f(\vec{r}, E'). \quad (51)$$

1 By substituting Eqs. (40)–(43) into Eqs. (28)–(30), the saturation values based on the  
 2 fundamental mode approximation can be rewritten as follows:

$$Y_\infty \approx \left( \frac{\mathcal{D}_0}{-\rho \mathcal{F}_1} \right) \left( \frac{\mathcal{F}_2}{-\rho \mathcal{F}_1} + \frac{\mathcal{S}_2}{\mathcal{S}_1} \right), \quad (52)$$

$$\mathcal{Y}_{3,\infty} \approx \left( \frac{\mathcal{D}_0}{-\rho \mathcal{F}_1} \right)^2 \left( \frac{\mathcal{F}_3}{-\rho \mathcal{F}_1} + \frac{\mathcal{S}_3}{\mathcal{S}_1} + 3 \frac{\mathcal{F}_2}{-\rho \mathcal{F}_1} \left( \frac{\mathcal{F}_2}{-\rho \mathcal{F}_1} + \frac{\mathcal{S}_2}{\mathcal{S}_1} \right) \right), \quad (53)$$

$$\mathcal{Y}_{4,\infty} \approx \left( \frac{\mathcal{D}_0}{-\rho \mathcal{F}_1} \right)^3 \left( \frac{\mathcal{F}_4}{-\rho \mathcal{F}_1} + \frac{\mathcal{S}_4}{\mathcal{S}_1} + 6 \frac{\mathcal{F}_2}{-\rho \mathcal{F}_1} \left( \frac{\mathcal{F}_3}{-\rho \mathcal{F}_1} + \frac{\mathcal{S}_3}{\mathcal{S}_1} \right) + \left( 4 \frac{\mathcal{F}_3}{-\rho \mathcal{F}_1} + 15 \left( \frac{\mathcal{F}_2}{-\rho \mathcal{F}_1} \right)^2 \right) \left( \frac{\mathcal{F}_2}{-\rho \mathcal{F}_1} + \frac{\mathcal{S}_2}{\mathcal{S}_1} \right) \right), \quad (54)$$

$$\mathcal{S}_n \equiv \int_V dV S(\vec{r}) \sum_{q=0}^{\infty} \frac{q!}{(q-n)!} p_s(q, \vec{r}) \left( \bar{\psi}_{0,s}^\dagger(\vec{r}) \right)^n, \quad (55)$$

$$\bar{\psi}_{0,s}^\dagger(\vec{r}) \equiv \int_0^\infty dE' \int_{4\pi} d\Omega' \frac{\chi_s(\vec{r}, E')}{4\pi} \psi_0^\dagger(\vec{r}, E', \vec{\Omega}'). \quad (56)$$

3 From Eqs. (52)–(54), if  $-\rho < 0.1$  or  $0.9 < k_{\text{eff}} < 1$ , ratios of  $\mathcal{Y}_{3,\infty}/Y_\infty^2$  and  $\mathcal{Y}_{4,\infty}/Y_\infty^3$  can  
 4 be further approximated:

$$\frac{\mathcal{Y}_{3,\infty}}{Y_\infty^2} \approx 3 + \frac{\mathcal{F}_1}{\mathcal{F}_2} \left( \frac{\mathcal{F}_3}{\mathcal{F}_2} - 3 \frac{\mathcal{S}_2}{\mathcal{S}_1} \right) (-\rho), \quad (57)$$

$$\frac{\mathcal{Y}_{4,\infty}}{Y_\infty^3} \approx 15 + 10 \frac{\mathcal{F}_1}{\mathcal{F}_2} \left( \frac{\mathcal{F}_3}{\mathcal{F}_2} - 3 \frac{\mathcal{S}_2}{\mathcal{S}_1} \right) (-\rho), \quad (58)$$

5 where the magnitude of  $\frac{\mathcal{F}_1}{\mathcal{F}_2} \left( \frac{\mathcal{F}_3}{\mathcal{F}_2} - 3 \frac{\mathcal{S}_2}{\mathcal{S}_1} \right)$  is approximately less than 1 [17,20]. It is  
 6 interestingly noted that these ratios converge to constant values without depending on  $\mathcal{F}_n$  and  
 7  $\mathcal{S}_n$ , as  $k_{\text{eff}}$  approaches to unity:

$$\lim_{-\rho \rightarrow +0} \frac{\mathcal{Y}_{3,\infty}}{Y_\infty^2} \approx 3, \quad (59)$$

$$\lim_{-\rho \rightarrow +0} \frac{\mathcal{Y}_{4,\infty}}{Y_\infty^3} \approx 15. \quad (60)$$

1

2 Finally, on the basis of the above-mentioned discussion, it is assumed that the  
 3 magnitudes of  $\mathcal{Y}_3$  and  $\mathcal{Y}_4$  can be roughly approximated by the second and the third power  
 4 of  $Y$ , if  $-\rho < 0.1 = 10,000$  pcm:

$$\mathcal{Y}_3 \approx 3Y^2, \quad (61)$$

$$\mathcal{Y}_4 \approx 15Y^3, \quad (62)$$

5 Although errors exist between the true values of  $\mathcal{Y}_3$  and  $\mathcal{Y}_4$  and their approximations, using  
 6 the approximations seems to be better than completely neglecting  $\mathcal{Y}_3$  and  $\mathcal{Y}_4$ , or  $\mathcal{Y}_3 \approx$   
 7  $\mathcal{Y}_4 \approx 0$ . Thus, Eqs. (61) and (62) are utilized to discuss the importance of the second-order  
 8 neutron-correlation for estimating  $\sigma_Y$ . By substituting Eqs. (61) and (62) into Eqs. (26) and  
 9 (27), the third- and fourth-order factorial moments can be approximated using  $\langle C \rangle$  and the  
 10 second-order neutron-correlation value  $Y$ :

$$\langle C(C-1)(C-2) \rangle \approx \langle C \rangle^3 + 3Y\langle C \rangle^2 + 3Y^2\langle C \rangle, \quad (63)$$

$$\langle C(C-1)(C-2)(C-3) \rangle \approx \langle C \rangle^4 + 6Y\langle C \rangle^3 + 15Y^2\langle C \rangle^2 + 15Y^3\langle C \rangle. \quad (64)$$

11 From Eqs. (63) and (64), the following approximation formulae for the third- and fourth-order  
 12 central moments  $\mu_3$  and  $\mu_4$  can be obtained:

$$\mu_3 \approx (3Y^2 + 3Y + 1)\langle C \rangle, \quad (65)$$

$$\mu_4 \approx 3(Y+1)^2\langle C \rangle^2 + (15Y^3 + 18Y^2 + 7Y + 1)\langle C \rangle. \quad (66)$$

13 By substituting Eqs. (65) and (66) into Eqs. (5)–(8) and approximating as  $\langle C \rangle \approx \bar{C}$ , the  
 14 simplified formula for the statistical error  $\sigma_{Y,2nd}$  can be finally derived as follows:

$$\sigma_{Y,2nd} \approx (Y + 1) \sqrt{\frac{Y(2Y + 1)(5Y + 2)}{N(Y + 1)^2 \bar{C}} + \frac{2}{N - 1}}. \quad (67)$$

1

2        If  $Y \approx 0$  in Eq. (67), *i.e.*, the probability distribution of neutron counts is sufficiently  
 3 approximated by the Poisson distribution, the statistical error  $\sigma_{Y,P}$  is guessed by the  
 4 following simple formula:

$$\sigma_{Y,P} \approx \sqrt{\frac{2}{N - 1}}. \quad (68)$$

5 By comparing Eq. (67) with Eq. (68), the statistical error  $\sigma_Y$  is corrected due to the  
 6 second-order neutron-correlation value  $Y$ .

7        Using Eq. (67), the statistical error  $\sigma_{Y,2nd}$  can be approximately estimated by reusing  
 8 the  $Y$  value without calculation of  $h_3$  and  $h_4$ , *i.e.*, the calculations of  $\bar{C}$  and  $s^2$  are  
 9 sufficient for the error estimation. In addition, Eq. (67) provides useful knowledge about the  
 10 statistical error of  $Y$ . For example, if the Feynman- $\alpha$  experiment is conducted under a  
 11 situation where the sample mean  $\bar{C}$  is large enough to satisfy  $\bar{C} \gg \frac{(N-1)Y(2Y+1)(5Y+2)}{2N(Y+1)^2}$ ,  $\sigma_{Y,2nd}$   
 12 can be mainly reduced by increasing  $N$  or total measurement time  $NT$ . Under such a  
 13 condition, a high strength external neutron source, or large  $\bar{C}$ , contributes little to improving  
 14 the statistical error of  $Y$ , although the relative statistical error of mean  $\langle \frac{\sigma_{\bar{C}}}{\bar{C}} \rangle$  can be reduced.  
 15 Note that the relative statistical error  $\langle \frac{\sigma_{Y,2nd}}{Y} \rangle$  can be reduced by increasing  $Y$  using a detector  
 16 with higher efficiency, as the absolute value of  $Y$  is proportional to the detection efficiency.  
 17 Hence, improvement of the detection efficiency is important for reducing the relative error of  
 18  $Y$  value.

19

### 1 3. Bootstrap method

#### 2 3.1. Bootstrap statistical error of $Y$ value

3 In our previous study, the statistical error estimation for the Feynman- $\alpha$  method using  
4 the bootstrap method was proposed [9]. The bootstrap method enables us to easily estimate  
5 statistical errors of both  $Y$  and the prompt neutron decay constant  $\alpha$ , by resampling using an  
6 experimentally inferred probability distribution of neutron count. In this study, the procedures  
7 are improved to effectively calculate the covariance of  $Y(T)$  between different gate widths  
8  $T$ , or the “bootstrap covariance matrix  $\Sigma_Y^*$ .” The improved procedures of the bootstrap  
9 method are explained below:

- 10 1. Original time-series data of neutron counts  $\vec{C}(T_0) = \{C_1, C_2, \dots, C_{N_0}\}$  are provided by a  
11 single measurement of reactor noise, where the basic counting gate width is  $T_0$ ; the total  
12 number of count data is  $N_0$ .
- 13 2. An upper limit value of bunching is set to  $K$ , where  $1 < K < N_0$ .
- 14 3. An empty vector  $\vec{C}^*(T_0) = \{\}$  is prepared ( $i = 1$ ).
- 15 4. The “resampling position  $\xi_i$ ” is determined using a uniform random integer number,  $1 \leq$   
16  $\xi_i \leq (N_0 - K + 1)$ . Then, successive time-series data  $\vec{C}_{\xi_i} = \{C_{\xi_i}, C_{\xi_i+1}, \dots, C_{\xi_i+K-1}\}$  are  
17 extracted from the original time series data, and added at the end of the vector  $\vec{C}^*(T_0)$ .  
18 This extraction of successive data is important to estimate the covariance of  $Y(T)$ .
- 19 5. As shown in Fig. 1, a “bootstrap sample of time-series data  $\vec{C}^*(T_0)$ ” is newly generated by  
20 repeating  $L = \lceil N_0/K \rceil$  times of random-resampling described in step 4:

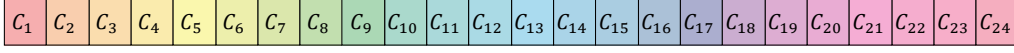
$$\vec{C}^*(T_0) = \{\vec{C}_{\xi_1}, \vec{C}_{\xi_2}, \dots, \vec{C}_{\xi_L}\}. \quad (69)$$

21 Note that extra data in  $\vec{C}_{\xi_L}$  is removed so that the total number of count data in  $\vec{C}^*(T_0)$  is  
22 equal to  $N_0$ , if necessary.

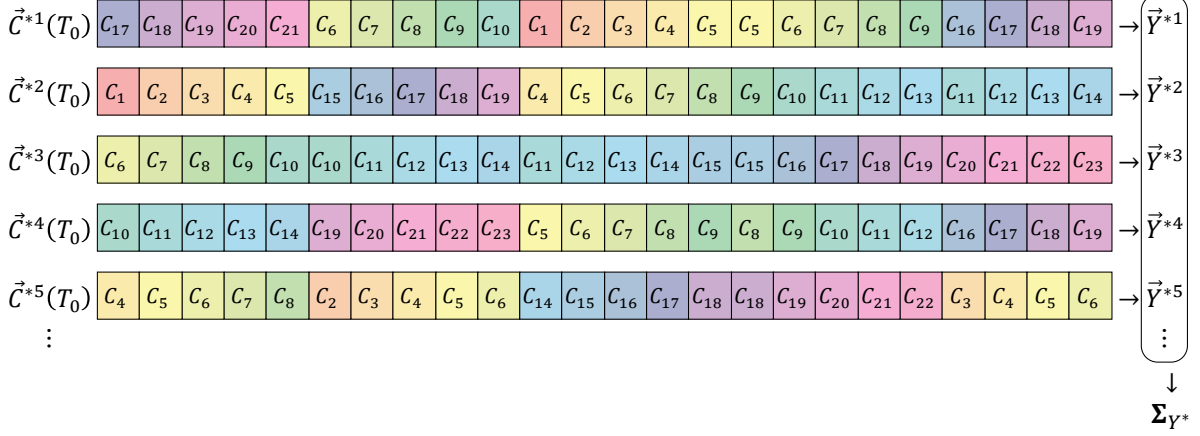
23



(a) original time-series data  $C(T_0)$



(b) bootstrap method



1

2

Figure 1. Example of bootstrap method for  $\Sigma_{Y^*}$  ( $N_0 = 24, K = 5$ )

3

4 6. By using Eq. (1) and applying an efficient bunching method to the bootstrap sample

5  $\vec{C}^*(T_0)$  in step 5, the variation in “bootstrap replicate  $Y^*(kT_0)$ ” is evaluated for the

6 bunching gate width  $kT_0$ , where  $k$  is the bunching number. To recursively apply the

7 bunching method to an already-bunched data, the bunching number  $k$  is given by  $k =$

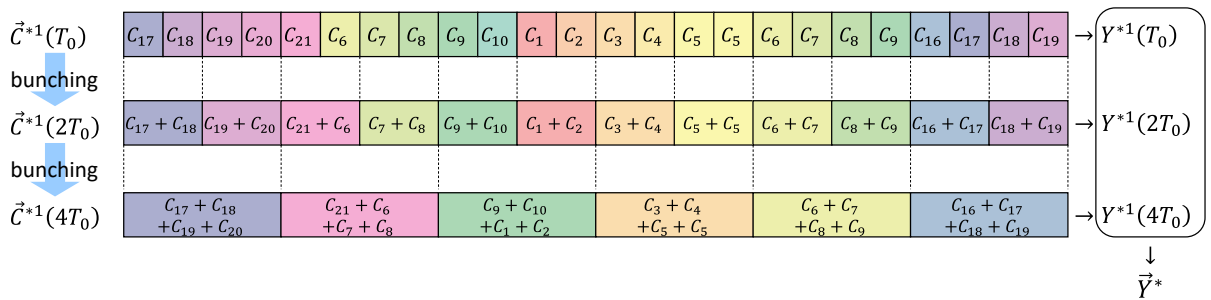
8  $p \times 2^j$  ( $j = 0, 1, \dots$ ), where  $p$  is an initial bunching number (e.g.,  $p =$

9  $2, 3, 5, 7, 9, 11, 13, 15, 17, 19$ ). As shown in Fig. 2,  $\vec{C}^*(2kT_0)$  is effectively produced by

10 combining a pair of successive elements in  $\vec{C}^*(kT_0)$ . Consequently, a row vector  $\vec{Y}^* =$

11  $\{Y^*(T_0), Y^*(2T_0), \dots, Y^*(KT_0)\}$  is obtained by this recursive bunching method.

12



13

14

Figure 2. Example of recursive bunching method ( $p = 2$ )

1

- 2 7. To estimate the covariance matrix of the bootstrap replicate  $\vec{Y}^*$ , steps 3–6 are repeated  
3  $B$  times. Consequently, a set of bootstrap replicates  $\vec{Y}^{*b}$  are obtained for  $b = 1, 2, \dots, B$ ,  
4 where  $B$  is the total number of bootstrap replicates.
- 5 8. Using the row vectors  $\vec{Y}^{*b}$ , the bootstrap covariance matrix  $\Sigma_{Y^*}$  is calculated as  
6 follows:

$$\Sigma_{Y^*} = \frac{1}{B-1} \sum_{b=1}^B (\vec{Y}^{*b} - \vec{Y}_{\text{ave}}^*)^T (\vec{Y}^{*b} - \vec{Y}_{\text{ave}}^*), \quad (70)$$

$$\vec{Y}_{\text{ave}}^* = \frac{1}{B} \sum_{b=1}^B \vec{Y}^{*b}, \quad (71)$$

7 where the bootstrap standard deviation  $\sigma_{Y^*}(kT_0)$  corresponds to the square root of the  
8 diagonal element in  $\Sigma_{Y^*}$ .

9

### 10 3.2. Bootstrap statistical error of prompt neutron decay constant

11 After step 8, the following additional procedures are necessary to estimate the statistical  
12 error of the prompt neutron decay constant  $\alpha$ :

- 13 9. Using the bootstrap covariance matrix  $\Sigma_{Y^*}$  in the least squares fitting process, the  
14 prompt neutron decay constant  $\alpha^{*b}$  is evaluated by fitting a model function of  $Y(T)$  to  
15 each value of  $\vec{Y}^{*b}$ . Consequently, bootstrap replicates  $\alpha^{*b}$  are obtained for  $b =$   
16  $1, 2, \dots, B$ .

- 17 10. As the result of step 9, a frequency distribution of  $\alpha^*$  is obtained. On the basis of this  
18 “bootstrap frequency distribution,” the percentile confidence interval (or 2.5 and 97.5  
19 percentile points) can be simply estimated to evaluate the range of the statistical error of  
20  $\alpha$ . Namely, the  $B$  bootstrap replicates  $\alpha^{*b}$  are sorted in ascending order. From the  
21  $(0.025 \times B)$ th and  $(0.975 \times B)$ th smallest values of sorted  $\alpha^{*b}$ , the lower and upper  
22 limits of 95% bootstrap confidence interval are simply estimated, respectively. If

1 necessary, the bootstrap standard deviation  $\sigma_{\alpha^*}$  can also be estimated as an indicator of  
 2 the statistical error of  $\alpha$ :

$$\sigma_{\alpha^*} = \frac{1}{B-1} \sqrt{\sum_{b=1}^B (\alpha^{*b} - \bar{\alpha}^*)^2}. \quad (72)$$

$$\bar{\alpha}^* = \frac{1}{B} \sum_{b=1}^B \alpha^{*b}. \quad (73)$$

3 Note that the 95% bootstrap confidence interval differs from the intervals of  $[\bar{\alpha}^* -$   
 4  $1.96\sigma_{\alpha^*}, \bar{\alpha}^* + 1.96\sigma_{\alpha^*}]$ , if the bootstrap frequency distribution is not well approximated  
 5 by a normal distribution.

6

## 7 **4. Experimental analysis**

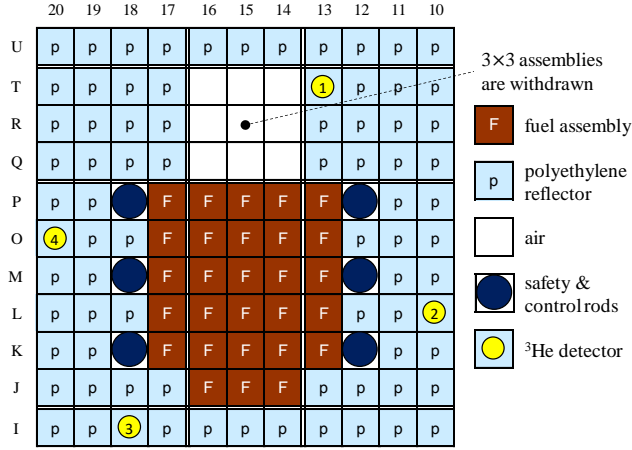
### 8 **4.1. Experimental conditions**

9 In our previous study, reactor noise experiments were conducted in the A-core  
 10 (A3/8”p36EU-NU) at the KUCA [9]. The experimental conditions are briefly explained  
 11 below.

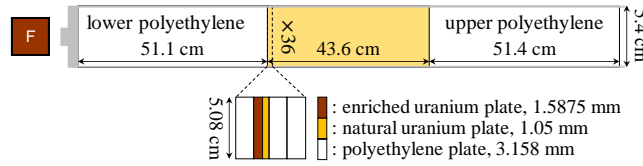
12 The experimental core and the loaded fuel assembly are shown in Figs. 3 and 4,  
 13 respectively. The core-average  $^{235}\text{U}$  enrichment was 5.4 wt%. Using MCNP6.2 [21] with  
 14 ENDF-B/VII.1 [22], core characteristics parameters were numerically estimated as follows:  
 15 Effective neutron multiplication factor  $k_{\text{eff}} = 0.93716 \pm 0.00003$ ; effective delayed neutron  
 16 fraction  $\beta_{\text{eff}} = 775 \pm 6$  [pcm]; and neutron generation time  $\Lambda = 42.04 \pm 0.04$  [ $\mu\text{s}$ ].  
 17 Consequently, subcriticality  $-\rho = 6705 \pm 3$  [pcm] and  $\frac{\beta_{\text{eff}} - \rho}{\Lambda} = 1779 \pm 2$  [1/s].

18 In this experiment,  $^3\text{He}$  detectors (#1–4) were placed at axially center positions of excore  
 19 reflector assemblies. Using these detectors, the time-series data of neutron counts were  
 20 successively measured. At the shutdown state, the reactor noise was measured without any  
 21 external neutron source such as Am-Be or Cf source, *i.e.*, using only the inherent neutron

1 source, which mainly consists of spontaneous fission of  $^{238}\text{U}$  and  $(\alpha,n)$  reactions of  $^{27}\text{Al}$  due to  
 2  $\alpha$ -decay of uranium isotopes [23]. Detector#2 was used for the present reactor noise analysis,  
 3 where the neutron count rate  $R = \bar{C}/T$  was  $4.444 \pm 0.011$  [count/s].



4  
 5 Figure 3. Top view of experimental core (A3/8”p36EU-NU).



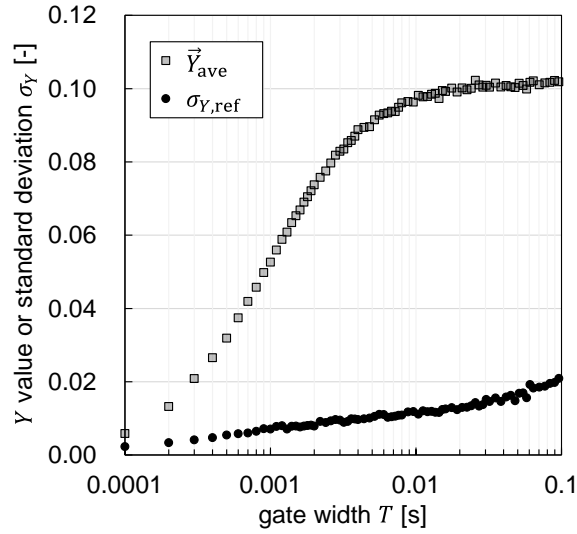
6  
 7  
 8 Figure 4. Fuel assembly loaded in experimental core.

9  
 10 To measure the reference value of the statistical error  $\sigma_{Y,\text{ref}}$ , reactor noise measurements  
 11 were repeated 93 times. Measurement time was 10 min for each measurement. Using the  
 12 recursive bunching method, the variation in  $Y(kT_0)$  was independently evaluated for each 10  
 13 min-measurement, where  $T_0 = 10^{-4}$  [s],  $N_0 = 6,000,000$ , and  $K = 1024$ . Thus, if the  
 14 bunching counting gate width is  $kT_0$ , the number of counting gate  $N_k$  corresponds to  $N_k =$   
 15  $[6,000,000/k]$ . Using 93 sets of  $\vec{Y}_m = \{Y_m(T_0), Y_m(2T_0), \dots, Y_m(KT_0)\}$ , the reference  
 16 covariance matrix  $\Sigma_{Y,\text{ref}}$  was estimated as

$$\Sigma_{Y,\text{ref}} = \frac{1}{93-1} \sum_{m=1}^{93} (\vec{Y}_m - \vec{Y}_{\text{ave}})^T (\vec{Y}_m - \vec{Y}_{\text{ave}}), \quad (74)$$

$$\vec{Y}_{\text{ave}} = \frac{1}{93} \sum_{m=1}^{93} \vec{Y}_m, \quad (75)$$

1 where the statistical error  $\sigma_{Y,\text{ref}}$  corresponds to the square root of the diagonal element in  
2  $\Sigma_{Y,\text{ref}}$  Figures 5 and 6 shows  $\vec{Y}_{\text{ave}}$  with the reference statistical error  $\sigma_{Y,\text{ref}}$  and the  
3 correlations of  $\Sigma_{Y,\text{ref}}$  (*i.e.*,  $(\text{diag}(\Sigma_{Y,\text{ref}}))^{-1/2} \Sigma_{Y,\text{ref}} (\text{diag}(\Sigma_{Y,\text{ref}}))^{-1/2}$ ), respectively. The  
4 measured  $Y$  values are less than approximately 0.1. In addition,  $Y(kT_0)$  are positively  
5 correlated between different gate widths  $kT_0$  due to the bunching method. The overall trend  
6 of Fig. 6 indicates that the correlations of  $Y(kT_0)$  become smaller as the difference between  
7  $kT_0$  and  $k'T_0$  increases. Because of the recursive bunching method, as shown in Fig. 2, the  
8 correlations between  $kT_0$  and  $2kT_0$  tend to become stronger.  
9



10

11

Figure 5.  $\vec{Y}_{\text{ave}}$  with reference statistical error  $\sigma_{Y,\text{ref}}$ .

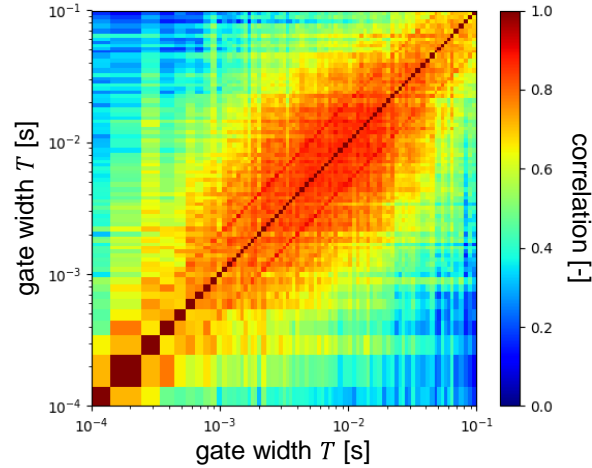


Figure 6. Correlations of the reference covariance matrix  $\Sigma_{Y,\text{ref}}$ .

To confirm the validity of the error estimation formulae, one of the 10 min-measurements was selected. Then, the statistical errors  $\sigma_{Y,h}$  and  $\sigma_{Y,2\text{nd}}$  were estimated by Eqs. (13) and (67), respectively. To better understand the second-order neutron-correlation effect, the approximated statistical error  $\sigma_{Y,p}$  based on the Poisson distribution was evaluated using Eq. (68). Furthermore, as an alternative error estimation technique, the bootstrap standard deviation  $\sigma_{Y^*}$  was also evaluated by the bootstrap method with  $B = 1000$ .

#### 4.2. Results of statistical error of $Y$

Figure 7 shows the reference  $\sigma_{Y,\text{ref}}$  and the following statistical errors for the 50<sup>th</sup> trial ( $m = 50$ ) of 10 min-measurement: (1)  $\sigma_{Y,p}$  based on the Poisson distribution, (2)  $\sigma_{Y,2\text{nd}}$  using the simplified formula by reusing the  $Y$  value, (3)  $\sigma_{Y,h}$  using the unbiased estimators for the third- and fourth-order central moments, and (4)  $\sigma_{Y^*}$  by the bootstrap method. The summary of statistical errors for  $1 \leq m \leq 93$  is shown in the attached mp4 file (sigmaY.mp4).

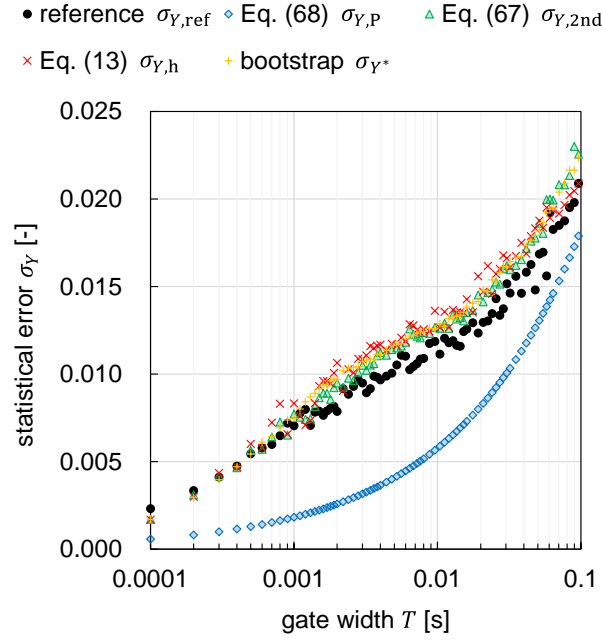


Figure 7. Estimation results of the statistical error of  $Y$  value ( $m = 50$ ).

As shown in Fig. 7,  $\sigma_{Y,2nd}$ ,  $\sigma_{Y,h}$ , and  $\sigma_{Y^*}$  agree well with reference  $\sigma_{Y,ref}$ . Compared with these results,  $\sigma_{Y,P}$  is significantly underestimated, although  $\sigma_{Y,P}$  is the simplest way to roughly guess the statistical error using only  $N$  without the measured neutron count data. By comparing  $\sigma_{Y,P}$  and  $\sigma_{Y,2nd}$ , it is confirmed that the second-order neutron-correlation effect is important for improving the estimation of the statistical error  $\sigma_Y$ . As  $\sigma_{Y,2nd}$  is nearly equal to  $\sigma_{Y,h}$ , it is demonstrated that the simplified formula of Eq. (67) is applicable to the experimental results in this study. Therefore, it seems to be reasonable that the third- and fourth-order neutron-correlation values can be approximated estimated by Eqs. (61) and (62). The advantage of  $\sigma_{Y,2nd}$  is convenience, *i.e.*, the statistical error can be obtained from the measurement values  $\bar{C}$  and  $Y$  only. Although  $\sigma_{Y,h}$  requires the additional calculation for  $h_3$  and  $h_4$ , the calculation cost is insignificant; thus  $\sigma_{Y,h}$  is also one of the practical estimation methods. Note that the statistical fluctuation of  $\sigma_{Y,h}$  seems to be larger owing to the use of higher-order central moments  $h_3$  and  $h_4$ .

1 As previously reported in reference [9], the bootstrap method enables reasonable  
2 estimation of statistical errors, such as the bootstrap standard deviation  $\sigma_{Y^*}$ . As shown in Fig.  
3 7,  $\sigma_{Y^*}$  and  $\sigma_{Y,h}$  are almost the same. The statistical fluctuation in  $\sigma_{Y^*}$  is relatively small  
4 because the total number of bootstrap replicates  $B$  is sufficiently large. The disadvantage of  
5 the bootstrap method is that calculation cost is relatively high owing to the resampling  
6 procedures. In the present analysis, the bootstrap replicates  $Y^*$  were randomly resampled  
7 1000 times to obtain  $\sigma_{Y^*}$  with high precision, thus the total calculation time of the bootstrap  
8 method is approximately at least 1000 times higher than that of  $\sigma_{Y,2nd}$  and  $\sigma_{Y,h}$ . Because of  
9 this calculation time, the bootstrap method may be unsuitable for real-time statistical error  
10 estimation in the on-line monitoring system.

11

### 12 **4.3. Discussion on the statistical error of the prompt neutron decay constant**

13 In the present study, theoretical formulae only for  $\sigma_Y$  were derived. The theoretical  
14 derivation for the statistical error of the prompt neutron decay constant  $\alpha$  (which is denoted  
15 by  $\sigma_\alpha$ ) is a challenging issue, because the derivation of  $\sigma_\alpha$  is more complicated owing to the  
16 fitting procedure for  $\alpha$ . In addition, as shown in Fig. 6, the  $Y$  values have correlations  
17 between different gate widths because of the bunching method. The derivation of a theoretical  
18 formula for the estimation of the covariance matrix  $\Sigma_Y$  is not straightforward.

19 Using the improved bootstrap method, however, the bootstrap covariance matrix  $\Sigma_{Y^*}$   
20 can be numerically evaluated as shown in Fig. 8. The summary of correlations of  $\Sigma_{Y^*}$  for  
21  $1 \leq m \leq 93$  is shown in the attached mp4 file (correlationY.mp4). By comparing  $\Sigma_{Y^*}$  with  
22 the reference correlations of  $\Sigma_{Y,ref}$  in Fig. 6, we can see that  $\Sigma_{Y^*}$  seems to be useful as an  
23 alternative to  $\Sigma_{Y,ref}$ .

24



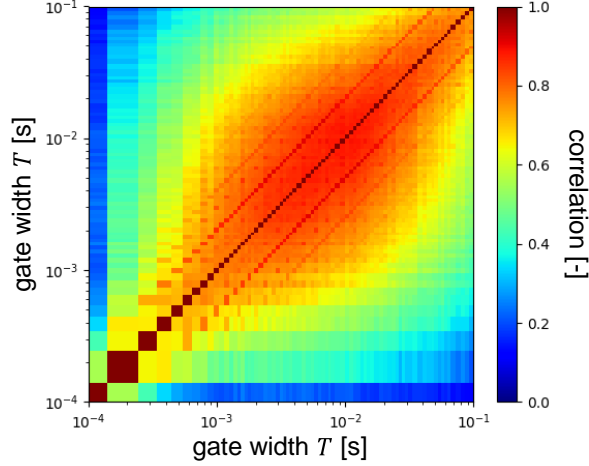


Figure 8. Correlations of bootstrap covariance matrix  $\Sigma_{Y^*}$  ( $m = 50$ ).

As a numerical study, the following two fitting procedures for  $\alpha$  were compared for each of the 10 min-measurements:

- (a) Fitting error method without correlation: Using the inverse of the statistical error  $\sigma_{Y,h}$  described by Eq. (13), *i.e.*,  $\frac{1}{\sigma_{Y,h}}$ , as the weight, the least squares fitting was performed to estimate the  $\alpha$  value. As will be discussed later, the absolute value of  $\sigma_{Y,h}$  was just used as is, *i.e.*,  $\sigma_{Y,h}$  was not scaled according to the  $\chi^2$  value after the fitting. Then, the estimated fitting error of  $\alpha$  (which is denoted as  $\sigma_{\alpha,fit}$ ) was used as an alternative to  $\sigma_{\alpha}$ . If the probability distribution of  $Y$  is approximated by a normal distribution and the correlations (off-diagonal elements) of  $\Sigma_Y$  do not have a large impact on the estimation of the fitting error, it is expected that the magnitude of the fitting error  $\sigma_{\alpha,fit}$  is reasonable as a candidate of the statistical error  $\sigma_{\alpha}$  because  $\sigma_{\alpha,fit}$  is evaluated by the propagation of uncertainty using the Jacobian matrix with the statistical error  $\sigma_{Y,h}$  [24]. By assuming a normal distribution for the probability distribution of  $\alpha$ , the 95% confidence intervals were approximated as the range of  $[\alpha - 1.96\sigma_{\alpha,fit}, \alpha + 1.96\sigma_{\alpha,fit}]$ .

- (b) Bootstrap method with correlation: Using the bootstrap covariance matrix  $\Sigma_{Y^*}$ , the 95% bootstrap confidence intervals were estimated to express the range of statistical

1 error of  $\alpha$  without the assumption of normality for  $Y$ , as described in Section 3.2.

2 The bootstrap standard deviation  $\sigma_{\alpha^*}$  was also estimated and compared with  $\sigma_{\alpha, \text{fit}}$ .

3

4 To mainly evaluate  $\alpha$ , the following model function was used in the least squares fitting

5 [9]:

$$Y(T) \approx Y_{\infty} \left( 1 - \frac{1 - \exp(-\alpha T)}{\alpha T} \right) + A T + B, \quad (76)$$

6 where  $Y_{\infty}$  is the saturation value, and  $A$  and  $B$  are supplemental fitting parameters to

7 correct the spatial and neutron-energetic higher-order modes, the delayed neutron and the

8 dead-time effects, respectively. Owing to their effects, a more rigorous theoretical expression

9 of  $Y(T)$  can be expressed as

$$Y(T) \approx \sum_{n=0}^{\infty} Y_{p,n,\infty} \left( 1 - \frac{1 - \exp(-\alpha_n T)}{\alpha_n T} \right) + \sum_{i=1}^6 Y_{d,i,\infty} \left( 1 - \frac{1 - \exp(-\omega_i T)}{\omega_i T} \right) - 2R\tau, \quad (77)$$

10 where the first, second, and third terms on the right-hand side correspond to terms due to

11 spatial and neutron-energetic modes [17], delayed neutrons [25], and dead-time  $\tau$  [26],

12 respectively;  $\alpha_n$  is the  $n$ th mode of the prompt neutron decay constant (the fundamental

13 mode corresponds to  $n = 0$ );  $\omega_i$  indicates the decay constant due to a delayed neutron;

14  $Y_{p,n,\infty}$  and  $Y_{d,i,\infty}$  are saturation values for each component with respect to  $\alpha_n$  and  $\omega_i$ . Note

15 that the decay constants satisfy the following conditions:  $\omega_i \ll \alpha_0$  and  $\alpha_0 < \alpha_1 < \alpha_2 < \dots$ .

16 In the fitting process, a complicated formula does not necessarily yield a good fitting result

17 owing to the overfitting issue. In this study, thus, we utilized the simplified fitting formula of

18 Eq. (76) instead of Eq. (77). To simplify the fitting formula, let us assume  $\omega_i T \ll 1$  and

19  $\alpha_n T \gg 1$ . Then Eq. (77) can be approximated as

$$Y(T) \approx Y_{p,0,\infty} \left( 1 - \frac{1 - \exp(-\alpha_0 T)}{\alpha_0 T} \right) + \sum_{i=1}^6 \left( \frac{1}{2} Y_{d,i,\infty} \omega_i \right) T + \sum_{n=1}^{\infty} Y_{p,n,\infty} - 2R\tau. \quad (78)$$

1 Thus, the fitting parameters  $A$  and  $B$  in Eq. (76) correspond to  $\sum_{i=1}^6 \left(\frac{1}{2} Y_{d,i,\infty} \omega_i\right)$  and  
2  $\sum_{n=1}^{\infty} Y_{p,n,\infty} - 2R\tau$ , respectively.

3 In this study, “scipy.optimize.curve\_fit” was utilized for the non-linear least squares  
4 fitting [27]. In the module of “scipy.optimize.curve\_fit,” the option of “absolute\_sigma” was  
5 explicitly set to “True” in order to simply use the absolute value of  $\sigma_{Y,h}$  as in the estimation  
6 of  $\sigma_{\alpha,\text{fit}}$ . In the default setting of “absolute\_sigma=False,” the  $\chi^2$  value after the fitting was  
7 normalized to be equal to the number of freedoms, which corresponds to  
8 (total number of  $Y(kT_0)$ ) – (total number of fitting parameters) . The option of  
9 “absolute\_sigma” influences the fitting error and has no impact on procedure (b) because the  
10 95% bootstrap confidence interval and  $\sigma_{\alpha^*}$  are calculated from 1000 fitting values of  $\alpha^*$  in  
11 the bootstrap method.

12 Figure 9 shows the estimated 95% confidence intervals obtained by using the two fitting  
13 procedures (a) and (b). In Fig. 9, the black dashed horizontal line represents the sample mean  
14 of 93 trial values of  $\alpha$ ; and a dark-colored plot indicates that the sample mean exists out of  
15 the estimated 95% confidence interval. As results of procedures (a) and (b) for 93 trials ( $1 \leq$   
16  $m \leq 93$ ), the sample means of the 93 fitting values  $\alpha_m$  (which is denoted as  $\bar{\alpha}$ ) were 1764  
17 and 1772 [1/s], respectively, while the standard deviations of the 93 fitting values  $\alpha_m$  (which  
18 is denoted as  $\sigma_{\alpha,\text{ref}}$ ) were 324 and 252 [1/s] (which are regarded as the reference values of  
19  $\sigma_{\alpha}$  for each procedure), respectively. Owing to the difference in the fitting procedure, there  
20 are differences in the fitting results between procedures (a) and (b). The sample means  $\bar{\alpha}$  are  
21 nearly equal to the numerical results of  $\frac{\beta_{\text{eff}} - \rho}{\Lambda} = 1779 \pm 2$  [1/s] using MCNP6.2 with  
22 ENDF-B/VII.1; thus, it was confirmed that the simplified fitting formula of Eq. (76) was  
23 reasonably applicable to the estimation of  $\alpha$  in this experimental analysis.

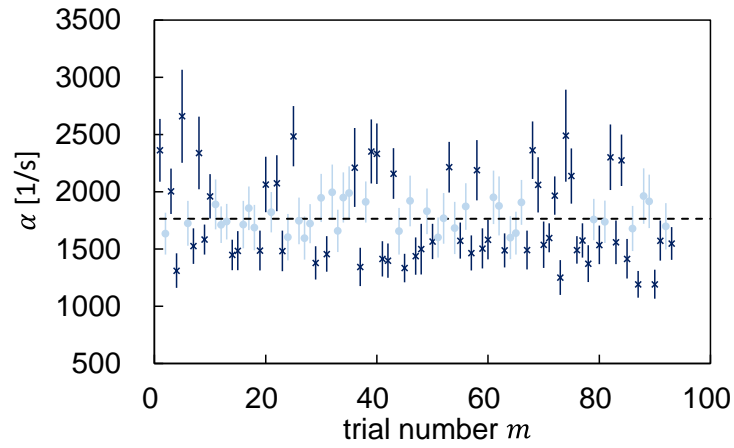
24 As can be seen from Fig. 9, the widths of 95% confidence intervals statistically fluctuate.  
25 For procedures (a) and (b), the sample means of 93 fitting errors  $\sigma_{\alpha,\text{fit},m}$  and 93 bootstrap  
26 standard deviations  $\sigma_{\alpha^*,m}$  were 238 and 272 [1/s], respectively. By comparing it with  $\sigma_{\alpha,\text{ref}}$ ,

1 the statistical error of  $\alpha$  estimated by procedure (a) seems to be slightly underestimated.  
2 Note that, if “absolute\_sigma” is set to “False” in procedure (a), the estimated statistical error  
3  $\sigma_{\alpha,\text{fit}}$  is significantly underestimated (sample mean of  $\sigma_{\alpha,\text{fit},m} \approx 102$  [1/s]), as shown in the  
4 Fig. 9-(i). Consequently, it was confirmed that  $\sigma_{Y,h}$  should not be scaled according to the  $\chi^2$   
5 value after the fitting in procedure (a) to avoid the underestimation of the statistical error  
6  $\sigma_{\alpha,\text{fit}}$ . This fact implies that the  $\chi^2$  test without correlation is useless to judge the goodness of  
7 fit.

8 To discuss the validity of the estimated 95% confidence intervals, we considered the  
9 coverage probability that the sample mean  $\bar{\alpha}$  exists within the range of the estimated 95%  
10 confidence interval. The coverage probability of procedures (a) and (b) were  $83/93 \approx 89\%$   
11 and  $87/93 \approx 94\%$ , respectively. The coverage probability of procedure (b) was slightly  
12 closer to 95% than that of procedure (a). Thus, to accurately evaluate the confidence interval  
13 for the statistical error of  $\alpha$ , it seemed that procedure (b) was slightly better than procedure  
14 (a), although procedure (a) could approximately guess the order of magnitude of statistical  
15 error  $\sigma_{\alpha}$  in this experimental analysis.

16 Consequently, a comparison of the fitting procedures (a) and (b) implied that the  
17 correlations of  $\Sigma_Y$  could be negligible for the order estimation of the statistical error  $\sigma_{\alpha}$ . To  
18 improve the coverage probability of the estimated confidence intervals, a more rigorous  
19 treatment of the correlations of  $\Sigma_Y$  might be important. However, the theoretical approach  
20 for the estimation of  $\Sigma_Y$  is still an open problem. On the other hand, although the bootstrap  
21 method is based on the numerical approach,  $\Sigma_Y$  can be numerically estimated from a single  
22 measurement of reactor noise; furthermore, the 95% confidence interval can be reasonably  
23 estimated without the assumption of normality.

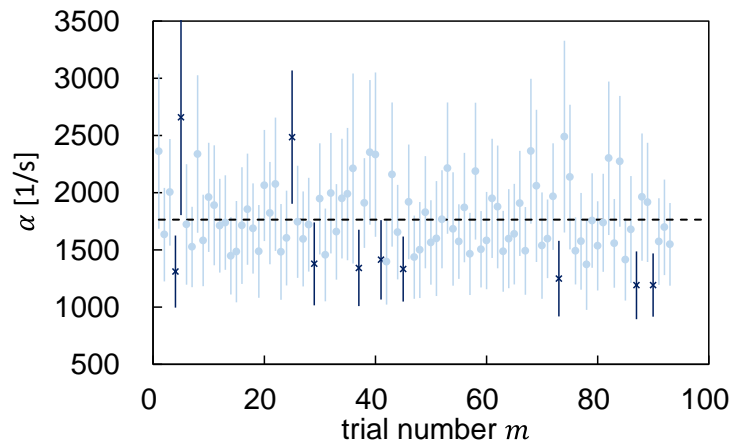
24



1

2

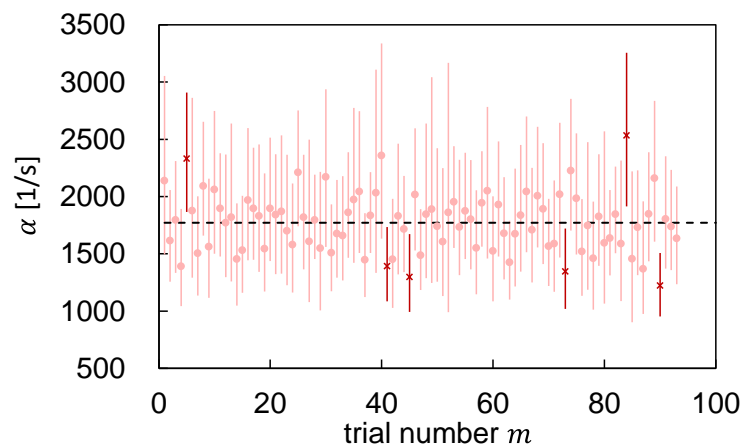
(i) Fitting error method without correlation (absolute\_sigma=False)



3

4

(ii) Fitting error method without correlation (absolute\_sigma=True)



5

6

(iii) Bootstrap method with correlation

7

Figure 9 Estimated 95% confidence interval of  $\alpha$ .

8

## 1 5. Conclusion

2 For the statistical error estimation of the  $Y$  value from a single measurement of reactor  
3 noise, the practical estimation formulae of  $\sigma_{Y,h}$  and  $\sigma_{Y,2nd}$  were derived by the propagation  
4 of uncertainty where the covariance between the sample mean and the unbiased variance is  
5 explicitly considered. The estimation of  $\sigma_{Y,h}$  requires additional calculations for the unbiased  
6 estimations of the third- and the fourth-order central moments,  $h_3$  and  $h_4$ . On the other hand,  
7  $\sigma_{Y,2nd}$  can be estimated by reusing the  $Y$  value without calculation of  $h_3$  and  $h_4$ . Note that  
8 the simplified formula of  $\sigma_{Y,2nd}$  is applicable under the fundamental mode approximation  
9 where the subcriticality is approximately less than 10,000 pcm.

10 In addition, the bootstrap method was improved to efficiently estimate the bootstrap  
11 covariance matrix  $\Sigma_{Y^*}$ . Using the improved bootstrap method, both the statistical error of  $Y$   
12 and the correlation of  $Y$  between different counting gate widths  $T$  due to the bunching  
13 method could be numerically obtained by the resampling based on a probability distribution  
14 that is experimentally inferred from a single measurement of reactor noise.

15 Through the reactor noise analysis for the actual KUCA experiment, it was validated that  
16 the statistical errors  $\sigma_{Y,h}$  and  $\sigma_{Y,2nd}$ , and the bootstrap standard deviation  $\sigma_{Y^*}$  agree well  
17 with the reference value of  $\sigma_{Y,ref}$ , which was obtained from multiple measurements of reactor  
18 noise. Furthermore, it was confirmed that the second-order neutron-correlation effect is  
19 important in the estimation of the statistical error of the  $Y$  value by comparison between  
20  $\sigma_{Y,2nd}$  and the approximated statistical error  $\sigma_{Y,P}$  using the Poisson distribution. Compared  
21 with the bootstrap method, the practical estimation formulae of  $\sigma_{Y,h}$  and  $\sigma_{Y,2nd}$  are more  
22 advantageous owing to their lower calculation cost.

23 To investigate the impact of correlations of  $\Sigma_Y$  on the statistical error of the prompt  
24 neutron decay constant  $\alpha$ , the following two fitting procedures were compared: the fitting  
25 error method using  $\sigma_{Y,h}$  without correlation and the bootstrap method with correlation using  
26  $\Sigma_{Y^*}$ . As a result, in the case of this experimental analysis, it was confirmed that the fitting

1 error method without correlation could be useful for the order estimation of the statistical  
2 error of  $\alpha$ . To avoid significant underestimation of statistical error,  $\sigma_{Y,h}$  should not be scaled  
3 according to the  $\chi^2$  value after the fitting. Compared with the fitting error method without  
4 correlation, the bootstrap method with correlation seems to be slightly better from the  
5 viewpoint of the coverage probability of the estimated confidence intervals. Thus,  
6 consideration of the correlations of  $\Sigma_Y$  might be important to improve the coverage  
7 probability; however, the theoretical approach for the estimation of  $\Sigma_Y$  is still an open  
8 problem.

## 1 **Acknowledgement**

2 This work has been carried out in part under the Visiting Researcher's Program of the  
3 Research Reactor Institute, Kyoto University. The authors are grateful to all the technical staff  
4 of KUCA for their assistance during the experiment. This work was supported by JSPS  
5 KAKENHI Grant-in-Aid for Young Scientists (B) (Grant Number 15K18317 and 17K14909).

## 7 **References**

- 8 1. Pyeon, C.H., Yamanaka, M., Endo, T., *et al.*, 2017. Experimental benchmarks on kinetic  
9 parameters in accelerator-driven system with 100 MeV protons at Kyoto University  
10 Critical Assembly. *Ann. Nucl. Energy.* 105, 346–354. DOI:  
11 [10.1016/j.anucene.2017.03.030](https://doi.org/10.1016/j.anucene.2017.03.030)
- 12 2. Pyeon, C.H., Yamanaka, M., Kim, S.H., *et al.*, 2017. Benchmarks of subcriticality in  
13 accelerator-driven system at Kyoto University Critical Assembly. *Nucl. Eng. Technol.* 49,  
14 1234–1239, DOI: [10.1016/j.net.2017.06.012](https://doi.org/10.1016/j.net.2017.06.012)
- 15 3. 2018. IRID Annual Research Report 2017, International Research Institute for Nuclear  
16 Decommissioning. 26-27. [http://irid.or.jp/\\_pdf/pamphleth29\\_eng.pdf#page=15](http://irid.or.jp/_pdf/pamphleth29_eng.pdf#page=15)
- 17 4. Feynman, R.P., de Hoffmann, F., Serber, R., 1956. Dispersion of the neutron emission in  
18 U-235 Fission. *J. Nucl. Energy.* 3, 64–69. DOI: [10.1016/0891-3919\(56\)90042-0](https://doi.org/10.1016/0891-3919(56)90042-0)
- 19 5. Pázsit, I., Yamane, Y., 1998. The variance-to-mean ratio in subcritical systems driven by a  
20 spallation source. *Ann. Nucl. Energy.* 25, 667–676. DOI:  
21 [10.1016/S0306-4549\(97\)00117-5](https://doi.org/10.1016/S0306-4549(97)00117-5)
- 22 6. Pázsit, I., Kitamura, Y., Wright, J., *et al.*, 2005. Calculation of the pulsed Feynman-alpha  
23 formulae and their experimental verification. *Ann. Nucl. Energy*, 32, 986–1007. DOI:  
24 [10.1016/j.anucene.2004.12.007](https://doi.org/10.1016/j.anucene.2004.12.007)
- 25 7. Pázsit, I., Pál, L., 2008. *Neutron Fluctuations: A Treatise on the Physics of Branching*  
26 *Processes*. Elsevier, Oxford.



- 1 8. Efron, B., 1979, Bootstrap methods: another look at the Jackknife. *Ann. Statist.* 7, 1–26.  
2 DOI: [10.1214/aos/1176344552](https://doi.org/10.1214/aos/1176344552)
- 3 9. Endo, T., Yamamoto, A., Yagi, T., *et al.*, 2016. Statistical error estimation of the  
4 Feynman- $\alpha$  method using the bootstrap method. *J. Nucl. Sci. Technol.* 53, 1447–1453.  
5 DOI: [10.1080/00223131.2015.1113898](https://doi.org/10.1080/00223131.2015.1113898)
- 6 10. Szeless, A., Ruby, L., 1969, Reactor noise parameters by the maximum likelihood method,  
7 *Trans. Am. Nucl. Soc.* 12, 739–740.
- 8 11. Szeless, A., Ruby, L., 1971. The exact probability distribution of reactor neutron noise.  
9 *Nucl. Sci. Eng.* 45, 7–13. DOI: [10.13182/NSE71-A20340](https://doi.org/10.13182/NSE71-A20340)
- 10 12. Dubi, C., Kolin, A., 2016. Analytic derivation of the statistical error in the Feynman- $\alpha$   
11 method. *Ann. Nucl. Energy.* 88, 186–193. DOI: [10.1016/j.anucene.2015.11.003](https://doi.org/10.1016/j.anucene.2015.11.003)
- 12 13. Dubi, C., Kolin, A., Blaise, P., *et al.*, 2017. Experimental validation of analytic formulas  
13 for the statistical uncertainty in the Feynman- $\alpha$  method. *Ann. Nucl. Energy.* 106, 84–90.  
14 DOI: [10.1016/j.anucene.2017.03.031](https://doi.org/10.1016/j.anucene.2017.03.031)
- 15 14. Misawa, T., Shiroya, S., Kanda K., 1990. Measurement of prompt neutron decay constant  
16 and large subcriticality by the Feynman- $\alpha$  method. *Nucl. Sci. Eng.* 104, 53–65. DOI:  
17 [10.13182/NSE104-53](https://doi.org/10.13182/NSE104-53)
- 18 15. Dodge, Y., Rousson, V., 1999. The complications of the fourth central moment. *Am. Stat.*  
19 53, 267–269. DOI: [10.1080/00031305.1999.10474471](https://doi.org/10.1080/00031305.1999.10474471)
- 20 16. Rose, C., Smith, M.D., 2002. *Mathematical Statistics with Mathematica*. Springer-Verlag,  
21 New York, 253–256.
- 22 17. Endo, T., Yamane, Y., Yamamoto, A., 2006. Space and energy dependent theoretical  
23 formula for the third order neutron correlation technique. *Ann. Nucl. Energy.* 33, 521–  
24 537. DOI: [10.1016/j.anucene.2006.02.002](https://doi.org/10.1016/j.anucene.2006.02.002)
- 25 18. Endo, T., Yamane, Y., Yamamoto, A., 2006. Derivation of theoretical formula for the third  
26 order neutron correlation technique by using importance function. *Ann. Nucl. Energy.* 33,

- 1 857–868. DOI: [10.1016/j.anucene.2006.05.005](https://doi.org/10.1016/j.anucene.2006.05.005)
- 2 19. Endo, T., Yamamoto, A., Yamane, Y., 2008. Development of deterministic code based on  
3 the discrete ordinates method for the third-order neutron correlation technique. *Ann. Nucl.*  
4 *Energy.* 35, 927–936. DOI: [10.1016/j.anucene.2007.09.014](https://doi.org/10.1016/j.anucene.2007.09.014)
- 5 20. Gwin, R., Spencer R.R., Ingle R.W., 1984. Measurements of the energy dependence of  
6 prompt neutron emission from  $^{233}\text{U}$ ,  $^{235}\text{U}$ ,  $^{239}\text{Pu}$ , and  $^{241}\text{Pu}$  for  $E_n = 0.005$  to 10 eV relative  
7 to emission from spontaneous fission of  $^{252}\text{Cf}$ . *Nucl. Sci. Eng.* 87, 381–404. DOI:  
8 [10.13182/NSE84-A18506](https://doi.org/10.13182/NSE84-A18506)
- 9 21. Werner, C.J. (editor), 2017. MCNP User’s manual – code version 6.2, Los Alamos  
10 National Laboratory, LA-UR-17-29981.
- 11 22. Chadwick, M.B., Herman, M., Obložinský, P., *et al.*, 2011. ENDF/B-VII.1 nuclear data  
12 for science and technology: cross Sections, covariances, fission product yields and decay  
13 data. *Nucl. Data Sheets.* 112, 2887–2996. DOI: [10.1016/j.nds.2011.11.002](https://doi.org/10.1016/j.nds.2011.11.002)
- 14 23. Shiozawa, T., Endo, T., Yamamoto, A., *et al.*, 2015. Investigation on subcriticality  
15 measurement using inherent neutron source in nuclear fuel. JAEA-Conf 2014-003, Japan  
16 Atomic Energy Agency. DOI: [10.11484/jaea-conf-2014-003](https://doi.org/10.11484/jaea-conf-2014-003)
- 17 24. Bard, Y., 1974. *Nonlinear Parameter Estimation*. Academic Press, New York.
- 18 25. Williams, M.M.R., 1974. *Random Processes in Nuclear Reactors*. Pergamon, Oxford.
- 19 26. Hashimoto, K., Ohya, K., Yamane, Y., 1996. Experimental investigations of dead-time  
20 effect on Feynman- $\alpha$  method. *Ann. Nucl. Energy.* 23, 1099–1104. DOI:  
21 [10.1016/0306-4549\(95\)00121-2](https://doi.org/10.1016/0306-4549(95)00121-2)
- 22 27. 2017. SciPy Reference Guide Release 1.0.0. 1031–1034.  
23 <https://docs.scipy.org/doc/scipy-1.0.0/scipy-ref-1.0.0.pdf#page=1035>